Journal of
Synchrotron Radiation

ISSN 0909-0495

Received 2 March 2010
Accepted 13 December 2010

Time-resolved photoelectron spectroscopy using synchrotron radiation time structure

N. Bergeard,[a] M. G. Silly,[a] D. Krizmancic,[b] C. Chauvet,[a] M. Guzzo,[a,c] J. P. Ricaud,[a] M. Izquierdo,[a] L. Stebel,[d] P. Pittana,[d] R. Sergo,[d] G. Cautero,[d] G. Dufour,[e] F. Rochet[e] and F. Sirotti[a]*

[a]Synchrotron-SOLEIL, BP 48, Saint-Aubin, F91192 Gif sur Yvette Cedex, France, [b]Laboratorio TASC, IOM-CNR, SS 14 km 163.5, Basovizza, Trieste I-34149, Italy, [c]European Theoretical Spectroscopy Facility (ETSF), Laboratoire des Solides Irradiés (LSI), Ecole Polytechnique, CNRS, CEA-DSM, 91128 Palaiseau, France, [d]Sincrotrone Trieste SCpA, Strada Statale 14 km 163.5, Area Science Park, Basovizza, I-34012 Trieste, Italy, and [e]Laboratoire de Chimie Physique Matière et Rayonnement, Unité Mixte de Recherche CNRS 7614, Université Pierre et Marie Curie, 75231 Paris Cedex, France. E-mail: fausto.sirotti@synchrotron-soleil.fr

Synchrotron radiation time structure is becoming a common tool for studying dynamic properties of materials. The main limitation is often the wide time domain the user would like to access with pump–probe experiments. In order to perform photoelectron spectroscopy experiments over time scales from milliseconds to picoseconds it is mandatory to measure the time at which each measured photoelectron was created. For this reason the usual CCD camera-based two-dimensional detection of electron energy analyzers has been replaced by a new delay-line detector adapted to the time structure of the SOLEIL synchrotron radiation source. The new two-dimensional delay-line detector has a time resolution of 5 ns and was installed on a Scienta SES 2002 electron energy analyzer. The first application has been to characterize the time of flight of the photoemitted electrons as a function of their kinetic energy and the selected pass energy. By repeating the experiment as a function of the available pass energy and of the kinetic energy, a complete characterization of the analyzer behaviour in the time domain has been obtained. Even for kinetic energies as low as 10 eV at 2 eV pass energy, the time spread of the detected electrons is lower than 140 ns. These results and the time structure of the SOLEIL filling modes assure the possibility of performing pump–probe photoelectron spectroscopy experiments with the time resolution given by the SOLEIL pulse width, the best performance of the beamline and of the experimental station.

Keywords: time-resolved photoelectron spectroscopy; synchrotron radiation time structure; delay-line detector.

1. Introduction

Two-photon photoemission experiments are currently performed using short laser pulses to study ultra-fast phenomena. They are performed using the conventional pump and probe procedure. A laser pulse (pump pulse) excites an unoccupied state and a second laser pulse (probe pulse) ionizes this state and lifts the electron above the vacuum level. The accessible time resolution is a few femtoseconds. It has been used for lifetime measurements (Zhukov *et al.*, 2004), electron spin dynamics (Schneider *et al.*, 2006; Cinchetti *et al.*, 2006), dynamics and manipulation of adsorbate surface interaction (Yamamoto *et al.*, 2008), imaging potential states (Link *et al.*, 2001) and spin dynamics in Ni (Rhie *et al.*, 2003).

Studies on excited-state electronic structure range from femtochemistry (Bonn *et al.*, 1999; Hess *et al.*, 2002; Bauer *et al.*, 2001) to studies of dynamical interactions at surfaces (Long *et al.*, 2001*a*,*b*; Quast *et al.*, 1998) and to core excitations (Privalov *et al.*, 2003).

On third-generation synchrotron radiation sources the probe laser pulse is replaced by an X-ray pulse. In normal operation modes a time resolution of the order of 30 ps is currently achieved; a better time resolution is achieved in slicing experiments (Schoenlein *et al.*, 2000; Kachel *et al.*, 2007; Stamm *et al.*, 2007; Beaud *et al.*, 2009).

Although the obtainable time resolution with synchrotron radiation is lower than that of experiments performed with laser systems, higher and tunable photon energy allows a

complete determination of the electronic structure, and the perspective of working with shorter X-ray pulses from free-electron laser sources pushes the development of detectors and experimental set-up for new photoemission experiments.

At fourth-generation sources, pump–probe facilities with subpicosecond time resolution are under development where a high-power optical laser and a soft X-ray free-electron laser are combined.

The major difficulty to face is the precise synchronization of the two independent light sources. The solution can be given by commercial products from laser companies. Lasers for these pump–probe experiments are usually characterized by repetition rates ranging from 1 kHz to about 80 MHz. Synchrotron radiation in full-filling mode ('multibunch' mode) has repetition rates of some hundreds of MHz (500 MHz or 352 MHz for SOLEIL). At SOLEIL several specific injection configurations are available for time-resolved experiments: single-bunch mode with an interbunch time of 1.18 µs, eight-bunch mode with an interbunch distance of 145 ns, and a hybrid mode in which one-quarter of the bunches in the ring are replaced by a single bunch separated from the others by 145 ns. This hybrid mode is currently used also at ESRF (http://www.esrf.eu/Accelerators/Operation/Modes) and has the great advantage of delivering a 'normal' photon flux for all non-time-resolved experiments.

For many time-resolved experiments the laser repetition rate is significantly reduced in order to reach the photon density needed to excite a significant amount of the sample. Often the time window between two consecutive laser pulses is imposed by the relaxation time of the excited state. If the pump and the probe do not have the same frequency, a simple stroboscopic experiment is not possible and some gating technique must be applied to the detection system. The gating can be obtained, for example, by reducing the acceleration voltage of the detector microchannel plates. It remains in a waiting state and the required detection voltages are set only to the frequency of the pump.

The ideal measurement configuration for time-resolved experiments is to be compatible with the most common filling mode of the synchrotron radiation source: all the characterization prerogatives of an intense synchrotron radiation source are then available and the acquisition can be switched, when needed, to time-resolved experiments using the most effective electron energy analyser based on a high-resolution parallel two-dimensional detection system.

In photoelectron spectroscopy experiments the main problem comes from the long time period that the electrons spend in the electron energy analyser and from the jitter introduced by all the possible electron trajectories in the hemispherical analyser which can strongly spread the time of flight of the electrons. For modern analysers whose higher efficiency is based on parallel two-dimensional detection, times of flight of electrons with the same kinetic energy are expected to differ by several tens of nanoseconds (depending on kinetic energy, pass energy, lens mode, *etc.*).

If the detection system is fast enough, time-resolved experiments do not need a lower intensity filling mode of the synchrotron source. Gießel and co-workers showed that 1 ns time resolution can be obtained for a channeltron detection system (Gießel *et al.*, 2003). They worked on the voltage of the lenses and considered high pass energy values to perform time-resolved photoemission experiments with the BESSY synchrotron radiation source in full-filling mode.

We present here a new experimental set-up installed on the TEMPO beamline of the SOLEIL synchrotron radiation source. We modified a Scienta SES 2002 electron energy analyser, replacing the two-dimensional detection based on the presence of a phosphorous screen and a CCD camera with a delay-line two-dimensional detector, and the electronics studied to correlate each measuring event with the clock of the synchrotron radiation source to perform time-resolved experiments. The operating principle is based on previous experience in magnetization dynamics studies (Sirotti *et al.*, 2000) applied to photoelectron spectroscopy experiments.

2. Detector description

The most common detection system on high-resolution electron energy analysers is formed by microchannel plates (MCP) multiplication, phosphorous screen and CCD camera. We have replaced the Scienta detector stack by a delay-line detector in order to obtain direct electron counting.

The working principle of this detector is well known: two cross meander delay lines, deposited on alumina substrate, 'see' the pulse charge produced by the MCP and the impact position (on the MCP) is determined by measuring the time distance between the electromagnetic pulse arrival at the four extremities. The detector is essentially a preliminary version of the device described by Cautero *et al.* (2008), but not working in multi-hit mode and employing a z-stack in place of a chevron assembly.

The time resolution of the detector is provided by the correlation of each 'event' (acquisition of one electron) with the value of an externally triggered counter. As described in the next section, if the trigger is given by the pump and probe signals the time resolution is limited essentially by the counter performances. The actual detector counters are based on a FPGA (field-programmable gate array) able to count up to 200 MHz, allowing a time resolution of 5 ns. Although multi-hit acquisition is in principle also possible, allowing up to 27 ps resolution (TDC resolution), for the described experiments this acquisition mode is quite useless since the possible trajectories of the electrons inside the lenses and analyzer assembly can introduce 'jitters' that are higher by several tens of nanoseconds.

With respect to the version described by Cautero *et al.* (2008), the maximum count rate is limited to about 1.2×10^6 counts s^{-1} by the acquisition electronics and by the MCP configuration.

The behaviour of the detector as a function of the count rate is shown in Fig. 1. The count rate in fixed mode (y axis) is a function of the sample photocurrent when changing the beamline slit opening for constant photon energy. The real count rate was extracted from the sample current, extra-

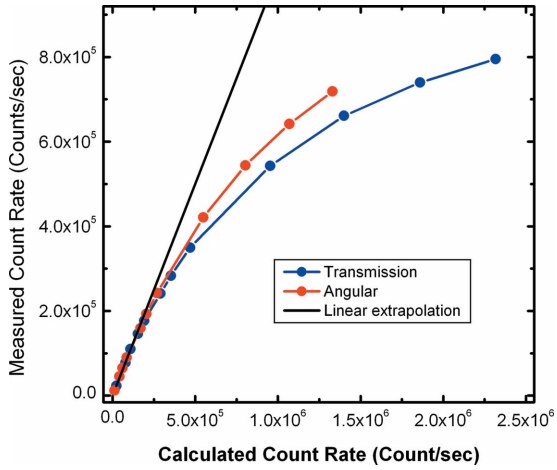

Figure 1
Linearity of the delay-line detector as a function of the count rate.

polating linearly the behaviour measured for low count rates. The difference between angular and transmission mode can be attributed to different electron densities on the detector area (because of the small focal spot the electrons are more localized on the detector in transmission mode) and is then due to a linearity problem of the MCP z-stack assembly as a function of the incoming electron flux.

A large effort was made to develop software to maintain the usual SES 2002 characteristics and allow our developments. The Scienta compatibility was obtained by writing a new library compatible with the Scienta software specifications which handles the detector. For normal photoelectron spectroscopy applications the new delay-line detection is completely transparent for the SES 2002 user: a window representing the intensity on the delay-line detector replaces the usual screen of the CCD camera. The delay-line detector library is fully compatible with the functions of the CCD camera.

When time-resolved experiments are performed, specific DLL saves multiple images of the detector independently of the Scienta SES 2002 software which always drives the high-voltage power supplies and applies all correction tables. In 'Fixed Scan' mode, it works synchronously with the SES scan. Two-dimensional images are here discriminated into predefined temporal intervals. A time histogram shows the time distribution of the collected electrons emitted from the sample. In 'Swept Mode', because of the large amount of three-dimensional data to be handled within swept scans, a disk swapping solution is being adopted. The swept data can be properly reconstructed later during the data treatment procedure. The medium disk amount for a swept scan is around 50 gigabits before reconstructing.

The detector can measure fast photoemission spectra at very high speed, limited only by reasons of statistics. In this case a sequence of fixed scans is launched while the timing gate is left open for a fixed amount of time, defined by the available memory. All these upgrades were possible thanks to the modularity of the Scienta software development.

In order to evaluate the performances in terms of energy and angular resolution, we show in Fig. 2 the angular-resolved

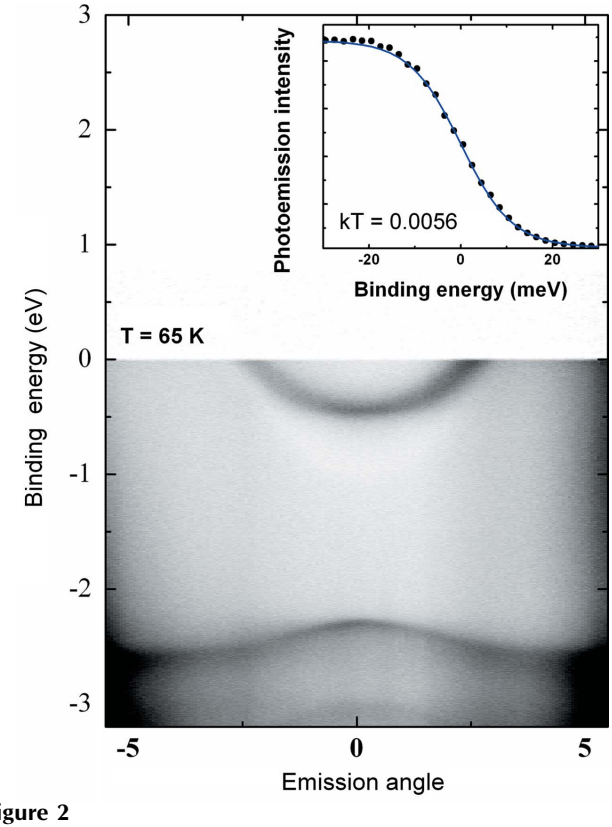

Figure 2
Angular-resolved photoemission experiment performed on a Au(111) clean and reconstructed surface measured with 50 eV photon energy and with the electron energy analyser in angular mode. The sample temperature was 65 K. The integrated photoemission intensity near the Fermi level (points) is compared in the inset with the Fermi function with kT = 0.0056.

photoemission measured in the valence band region of a Au(111) surface with 50 eV photon energy. The present detector has the same dimensions as the original MCP/phosphorous detector and can resolve 612 × 612 pixels. In order to optimize the time-dependent data transfer and data handling we decided to work with a detector resolving 306 × 306 pixels.

3. Time-resolved spectroscopy

SOLEIL synchrotron radiation source is characterized by the possibility of injecting 416 bunches separated by 2.84 ns. Two filling modes allow us to perform time-resolved photoelectron spectroscopy experiments: (i) the few-bunches mode, characterized by eight bunches, 50 ps wide, and separated by 148 ns; (ii) the hybrid mode, where three-quarters of the ring is completely filled and the other quarter is filled with a bunch with higher current separated from the full-filling region by 140 ns (http://www.synchrotron-soleil.fr/portal/page/portal/SourceAccelerateur/ModesFonctionnement). Time structure is normally used to perform pump and probe experiments where a laser or a magnetic pulse are the pump and the synchrotron radiation pulse is the probe. The pulses of the laser and of the synchrotron are synchronized, with a constant delay between the laser pulse and one of the synchrotron pulses. The laser pulse creates an excitation in the sample at

time $t = t_0$ and, if the lifetime is long enough, the synchrotron pulse takes a picture of the excited state at time t. By changing the delay between the two pulses the excitation and delay processes can be followed with a time resolution defined by the synchrotron pulse width.

When we measure photoemission spectra we must also consider the time the electrons spend in the analyser before reaching the detector and, even more important, the time spread of electrons having the same energy but different trajectories. In the case of two-dimensional detection spectra in a single detector image the characterization of the time behaviour of the analyser is a key point.

We performed this characterization measuring the time of flight of the electrons in the SES 2002 (http://www.vgscienta.com/productlist.aspx?IID=414) analyser as a function of kinetic energy, pass energy and angular or transmission mode. The probe time scale is now given by the detector time resolution (5 ns) and the synchrotron pulse is the triggering pulse event ejecting the electrons.

The experiments to test time-resolved behaviour were performed on a silicon sample protected by a thin oxide layer. On this sample we can set up the analyser to obtain the bulk Si-2*p* core level on the detector area as well as the Si-2*p* photoelectrons coming from the silica layer.

The image resulting on the SES 2002 detector in fixed mode is shown in Fig. 3 for 650 eV photon energy, a pass energy of 100 eV and with the analyser lens working in angular mode.

If the data acquisition on the detector is performed in time-resolved mode, the acquisition process is triggered by the SOLEIL synchrotron clock. When SOLEIL is operated in few-bunches mode the time period between identical pulses is 148 ns. With the detector time resolution of 5 ns, the total count rate represented in Fig. 3 can be decomposed in 30 images, each one corresponding to the intensity measured in a well defined time interval of 5 ns with respect to the photon

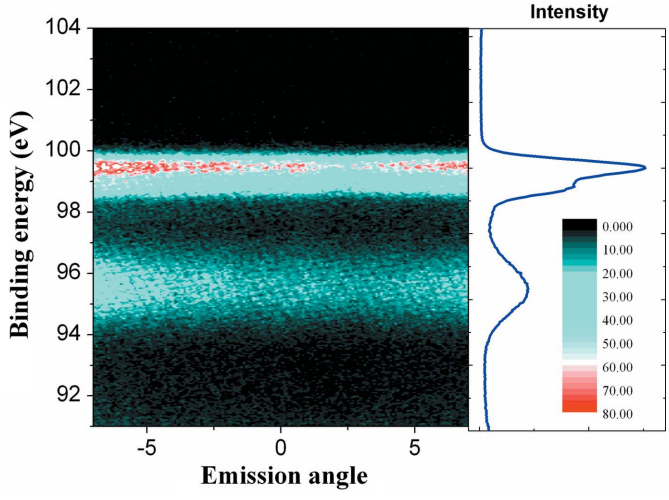

Figure 3
Detector image obtained by measuring the Si-2*p* core level of a SiO_2/Si(111) sample with a photon energy of 650 eV and a pass energy of 200 eV at normal emission in angular-resolved mode. The photoemission intensity spectrum obtained by integrating on the emission angle is shown on the right.

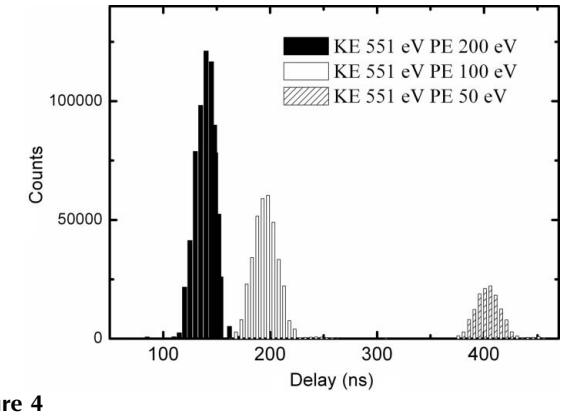

Figure 4
Time distribution of the photoelectron intensity measured as a function of the electron energy analyser pass energy for constant kinetic energy.

pulse trigger. This measurement of the time of flight of the electrons is presented by the time histogram appearing in the centre of Fig. 4. The photoelectrons reaching the detector with a pass energy of 100 eV and kinetic energy between 545 and 555 eV reach the detector in a time interval between 30 and 100 ns.

For this acquisition a time period of about 70 ns would be sufficient to associate each electron with the photon pulse which created it. For high kinetic energies and high pass energies the expected time distribution of the electrons is narrow but, when we move to very low kinetic and pass energies, we must verify that electrons created by different bunches can be discriminated at the detector level. The pump–probe photoemission experiments will be possible only for pass energies and kinetic energies for which the spread of the times of flight is lower than 148 ns.

The average arrival time depends strongly on the kinetic energies of the electrons and on the analyser pass energy. Fig. 4 shows the effect of the pass energy on the time detection of electrons having the same kinetic energy. Considering that the major part of the observed time spread results from the energy dependence of the flight times (Ulrich *et al.*, 2010), these time resolutions could be improved by considering the flight times with a two-dimensional kinetic energy.

The reduction of the pass energy results in a longer time of flight of the electrons, but the spread of the electrons entering the energy window transmitted by the analyser has a well defined Gaussian shape.

The time interval in which the electrons arrive at the analyser defines the minimum time interval needed in the photon source to separate these electrons. In Fig. 5 we compare the intensity distributions measured as a function of time for the fastest and slowest electrons. The white histogram is obtained for 200 eV kinetic energy electrons (200 eV pass energy, fast electrons) and for 20 eV kinetic energy electrons (2 eV pass energy, slow electrons). This latter configuration is the one which gives the best energy resolution of the electron energy analyser and still keeps a complete separation of the electrons produced by isolated SOLEIL bunches. In Fig. 6 the photoelectron intensity histograms are presented in the same interval to compare the time width of the electron distribution.

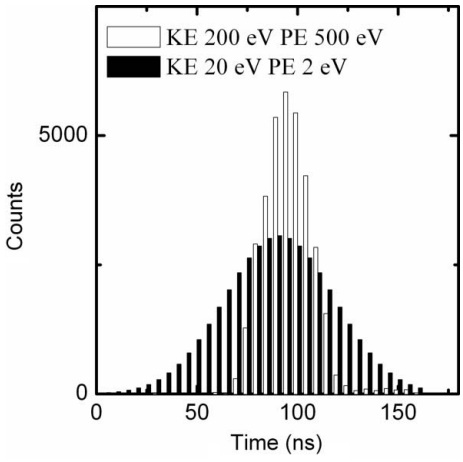

Figure 5
Photoelectron intensity distribution measured in each detector image with steps of 5 ns with respect to the photon pulse trigger. The white histogram is obtained for 200 eV kinetic energy and 500 eV pass energy (fast electrons) while the black histogram is obtained for 20 eV kinetic energy electrons and 2 eV pass energy of the electron energy analyser.

Even for very low pass energies and low kinetic energies the total distribution of the time of flight of the electrons is less than 200 ns. If a photon bunch is centred on an empty interval of at least 200 ns, the photoelectrons generated in the sample can be easily separated from the others.

When the SOLEIL synchrotron radiation source is operated in hybrid mode, an isolated bunch of higher intensity is injected into the centre of an empty interval of 240 ns. The bunch current of the hybrid mode is shown in the top panel of Fig. 6. The intensity of the isolated bunch is $\sim$8 mA. The other three-quarters of the ring are injected with smaller bunches of about 1 mA. The total current (stored in the machine) was at that time 200 mA. Improvements in the machine operation allow at present 500 mA to be injected and with the same time structure.

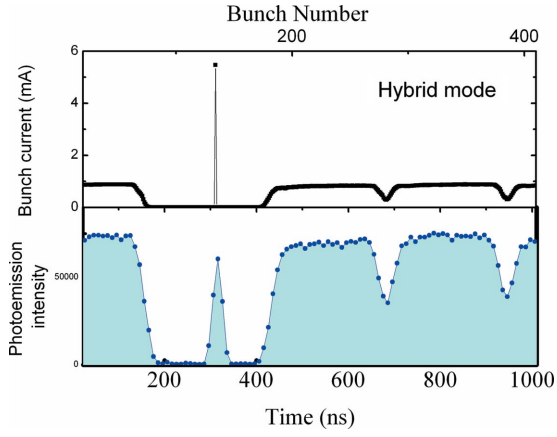

Figure 6
Time structure of the SOLEIL synchrotron radiation source when operating in the hybrid mode. The bunch current is reported as a function of the bunch number. The lower panel shows the photoemission intensity measured with the electron energy analyser operating in time-resolved mode.

At the TEMPO photoelectron spectroscopy experimental station we have used this time structure to calibrate the time delay introduced by changing the pass energy and the kinetic energy of the electron. A time spectrum is shown at the bottom of Fig. 6.

In this configuration the period of the source is longer and it is easier to measure the introduced delay with respect to the eight-bunches mode. In order to obtain a complete characterization of the time behaviour of the analyser we measured the position of the maximum of the Gaussian distribution for several pass energies (from 5 to 200 eV) as a function of the kinetic energy. The results are shown in Fig. 7. The absolute origin of the time scale was obtained by calculating the time of flight of fast electrons (500 eV at 500 eV pass energy) on a path corresponding to the average trajectory length in the electron energy analyser. The electrons' time of flight of the analyser in transmission mode is presented in panel Fig. 7(*a*), while the angular behaviour is shown in Fig. 7(*b*). The time of flight ranges between 100 ns and 1.2 µs. It is longer when the analyser is set to detect the emission angle of the photoelectrons.

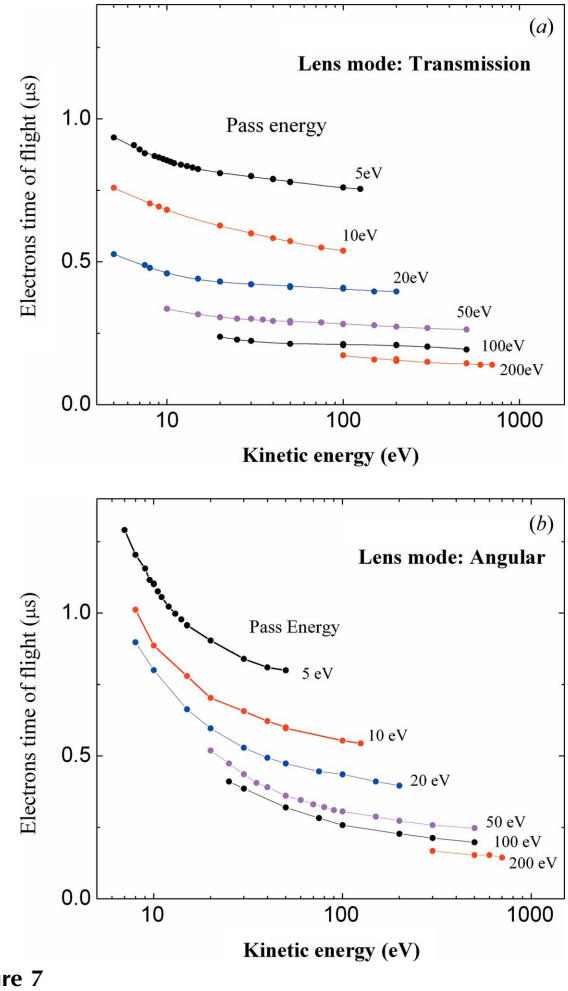

Figure 7
Photoelectrons' time of flight in the analyser as a function of the kinetic energy for all the pass energies (5, 10, 20, 50, 100, 200 eV) of the SES 2002 analyser measured for the two lens settings: transmission (*a*) and angular (*b*).

4. Conclusion

We have developed new equipment to perform time-resolved photoelectron spectroscopy using a synchrotron radiation time structure. The experimental set-up was tested using the time structure of the SOLEIL synchrotron radiation source in hybrid mode. The development is based on the installation of a two-dimensional delay-line detector replacing usual CCD cameras and by the development of dedicated electronics and software on a Scienta SES 2002 electron energy analyzer. The delay-line detector time resolution is 5 ns. As a first application we have characterized the time of flight of the photoemitted electrons in the analyzer as a function of their kinetic energy and the selected pass energy.

These results assure the possibility to separate the contribution of a single synchrotron radiation bunch and then perform pump–probe experiments using lasers and SOLEIL synchrotron radiation with selectable repetition rates. All experiments can be performed by taking advantage of the best performance of the beamline and of the electron energy analyzer and can be performed for all synchronous frequencies of the pump with respect to the probing frequency imposed by the synchrotron radiation.

If the synchrotron is operated in hybrid mode and using our new time-resolved two-dimensional detection system we can switch at any time between normal spectroscopy, highly effective because of the high photon flux of the full filling mode, and pump–probe experiments with all possible combinations of pump/probe frequency.

References

Bauer, M., Lei, C., Read, K., Tobey, R., Gland, J., Murnane, M. M. & Kapteyn, H. C. (2001). *Phys. Rev. Lett.* **87**, 025501.

Beaud, P., Johnson, S. L., Vorobeva, E., Staub, U., De Souza, R. A., Milne, C. J., Jia, Q. X. & Ingold, G. (2009). *Phys. Rev. Lett.* **103**, 155702.

Bonn, M., Funk, S., Hess, Ch., Denzler, D. N., Stampfl, C., Scheffler, M., Wolf, M. & Ertl, G. (1999). *Science*, **285**, 1042–1045.

Cautero, G., Sergo, R., Stebel, L., Lacovig, P., Pittana, P., Predonzani, M. & Carrato, S. (2008). *Nucl. Instrum. Methods Phys. Res. A*, **595**, 447–459.

Cinchetti, M., Sánchez Albaneda, M., Hoffmann, D., Roth, T., Wüstenberg, J.-P., Krauß, M., Andreyev, O., Schneider, H. C., Bauer, M. & Aeschlimann, M. (2006). *Phys Rev. Lett.* **97**, 177201.

Gießel, T., Bröcker, D., Schmidt, P. & Widdra, W. (2003). *Rev. Sci. Instrum.* **74**, 4620.

Hess, Ch., Wolf, M., Roke, S. & Bonn, M. (2002). *Surf. Sci.* **502–503**, 304–310.

Kachel, T., Holldack, K., Khan, S., Mitzner, R., Quast, T., Stamm, C. & Duerr, H. A. (2007). *AIP Conf. Proc.* **879**, 1250–1253.

Link, S., Dürr, H. A., Bihlmayer, G., Blügel, S., Eberhardt, W., Chulkov, E. V., Silkin, V. M. & Echenique, P. M. (2001). *Phys. Rev. B*, **63**, 115420.

Long, J. P., Chase, S. J. & Kabler, M. N. (2001*a*). *Chem. Phys. Lett.* **347**, 29–35.

Long, J. P., Chase, S. J. & Kabler, M. N. (2001*b*). *Phys. Rev. B*, **64**, 205415.

Privalov, T., Gelmukhanov, F. & Agren, H. (2003). *J. Electron Spectrosc. Relat. Phenom.* **129**, 43–54.

Quast, T., Bellmann, R., Winter, B., Gatzke, J. & Hertel, I. V. (1998). *J. Appl. Phys.* **83**, 1642.

Rhie, H.-S., Dürr, H. A. & Eberhardt, W. (2003). *Phys Rev. Lett.* **90**, 247201.

Schneider, H. C., Wüstenberg, J.-P., Andreyev, O., Hiebbner, K., Guo, L., Lange, J., Schreiber, L., Beschoten, B., Bauer, M. & Aeschlimann, M. (2006). *Phys. Rev. B*, **73**, 081302(R).

Schoenlein, R. W., Chattopadhyay, S., Chong, H. H. W., Glover, T. E., Heimann, P. A., Shank, C. V., Zholents, A. A. & Zolotorev, M. S. (2000). *Science*, **287**, 2237–2240.

Sirotti, F., Girlando, S., Prieto, P., Floreano, L., Panaccione, G. & Rossi, G. (2000). *Phys. Rev. B*, **61**, R9221–R9224.

Stamm, C., Kachel, T., Pontius, N., Mitzner, R., Quast, T., Holldack, K., Khan, S., Lupulescu, C., Aziz, E. F., Wietstruk, M., Dürr, H. A. & Eberhardt, W. (2007). *Nat. Mater.* **6**, 740–743.

Ulrich, V. *et al.* (2010). *J. Electron Spectrosc. Relat. Phenom.* doi:10.1016/j.elspec.2010.03.001.

Yamamoto, I., Mikamori, M., Yamamoto, R., Yamada, T., Miyakubo, K., Ueno, N. & Munakata, T. (2008). *Phys. Rev. B*, **77**, 115404.

Zhukov, V. P., Andreyev, O., Hoffmann, D., Bauer, M., Aeschlimann, M., Chulkov, E. V. & Echenique, P. M. (2004). *Phys. Rev. B*, **70**, 233106.